

Broadband ferromagnetic resonance linewidth measurement of magnetic tunnel junction multilayers

J. F. Sierra,¹ F. G. Aliev,¹ R. Heindl,^{2,a)} S. E. Russek,² and W. H. Rippard²

¹*Departamento Física de la Materia Condensada, C-III, Universidad Autónoma de Madrid, 28049 Madrid, Spain*

²*National Institute of Standards and Technology, Boulder, Colorado 80305, USA*

(Received 7 October 2008; accepted 1 December 2008; published online 7 January 2009)

The broadband ferromagnetic resonance (FMR) linewidth of the free layer of magnetic tunnel junctions is used as a simple diagnostic of the quality of the magnetic structure. The FMR linewidth increases near the field regions of free layer reversal and pinned layer reversal, and this increase correlates with an increase in magnetic hysteresis in unpatterned films, low-frequency noise in patterned devices, and previous observations of magnetic domain ripple by use of Lorentz microscopy. Postannealing changes the free layer FMR linewidth, indicating that considerable magnetic disorder, originating in the exchange-biased pinned layer, is transferred to the free layer.

© 2009 American Institute of Physics. [DOI: 10.1063/1.3054642]

Magnetic tunnel junctions (MTJs) are being developed for a variety of applications including magnetic recording sensors,¹ low-field magnetic sensors,² magnetic random-access memory,³ high-frequency spintronics devices,⁴ and logic devices.⁵ The quality of the MTJs depends sensitively on interfacial roughness, intermixing, and oxygen content, which in turn depend on materials used in the stack, deposition conditions, and annealing conditions. Ferromagnetic resonance (FMR) gives insight into both the magnetization dynamics and the quality of single ferromagnetic layers,⁶ multilayers,⁷ exchange-biased layers,⁸ and MTJs.⁹ The FMR linewidth depends on the intrinsic magnetic damping and extrinsic factors. The extrinsic factors include the presence of local moments, antiferromagnetic phases produced by a nonideal oxygen distribution near the tunnel barrier, and the presence of undesirable magnetic coupling—such as Néel coupling. Both the intrinsic and extrinsic dampings are important in determining switching times,¹⁰ oscillator linewidths,¹¹ and detector bandwidths in MTJ devices.⁴

Here, we present data using broadband FMR to characterize interfacial properties of MTJs at the wafer level and correlate regions of increased free-layer linewidth with the reversal of the free and pinned layers, the appearance of magnetization ripple, and increased $1/f$ noise. In this paper we define linewidth as the FMR linewidth of the free layer of the MTJ, and we have not measured the FMR response and the linewidth of the pinned layer of the MTJ.

The tunnel junctions were grown in a high-vacuum sputtering chamber on insulating quartz wafers for the FMR studies and on oxidized silicon for the device measurements. The structure of the MTJ wafers used for FMR measurements was [Ta(5 nm)\Cu(5 nm)\Ta(5 nm)\Ru(2 nm)\Ir₂₀Mn₈₀(10 nm)\Co₉₀Fe₁₀(3 nm)\Al₂O₃(1 nm)/Co₆₀Fe₂₀B₂₀(2 nm)/Ni₈₀Fe₂₀(23 nm)/Ta(3 nm)/Ru(7 nm)], where Co₉₀Fe₁₀(3 nm) forms the magnetic pinned layer. The wafers patterned into devices had a similar stack structure, except that the pinned layer was a Co₉₀Fe₁₀(2 nm)\Ru(0.85 nm)\Co₆₀Fe₂₀B₂₀(3 nm) synthetic

antiferromagnetic. The Co₆₀Fe₂₀B₂₀(2 nm)\Ni₈₀Fe₂₀(23 nm) forms the free layer that is studied here. All wafers were annealed at 250 °C in vacuum for 1 h in an applied magnetic field of 20 mT (these will be referred to “as deposited”). Some samples were further annealed in air for 1 h in an applied magnetic field of 100 mT along the same direction as the deposition field. In this study, we present data from four coupons obtained from the same MTJ FMR wafer: an as-deposited sample, a 250 °C annealed sample, a 275 °C annealed sample, and a 300 °C annealed sample, as well as data from one wafer with MTJ devices that are used for resistance noise measurements.

The high-frequency magnetization dynamics were measured by use of a commercial vector network analyzer (VNA) operating at frequencies up to 20 GHz. A VNA-FMR inductive technique was used to determine the FMR frequency and frequency swept linewidth Δf (full width at half maximum of the peak in the imaginary part of the susceptibility).¹² The FMR of the MTJ free layer was excited by a microwave magnetic field above a coplanar waveguide whose frequency was swept using the excitation signal from the VNA. The FMR spectra were obtained for different values of an applied in-plane magnetic field H_{ap} [see Fig. 2(b) inset], and normalized to a reference spectrum taken at a field such that the FMR resonance is outside the frequency range of interest. The reference fields serve also as the initialization field, which resets the magnetization to a well defined state before each measurement. Both positive- and negative-going field sweeps were obtained in which the initialization/reference fields are antialigned and aligned with the pinned direction, respectively. Note that at each value of H_{ap} a frequency swept FMR measurement was obtained and no field swept FMR spectra were measured. The absorption peaks were fitted to a resonance model in which the real and imaginary parts were fitted simultaneously.¹² The quasistatic magnetization characteristics were measured with a vibrating sample magnetometer. All measurements were performed at room temperature.

Figure 1 shows the resistance of a 64-element MTJ bridge as a function of applied magnetic field along with the resistance noise measured at 10 Hz (the applied voltage was

^{a)}Author to whom correspondence should be addressed. Tel.: 303-497-4224. Electronic mail: heindl@nist.gov.

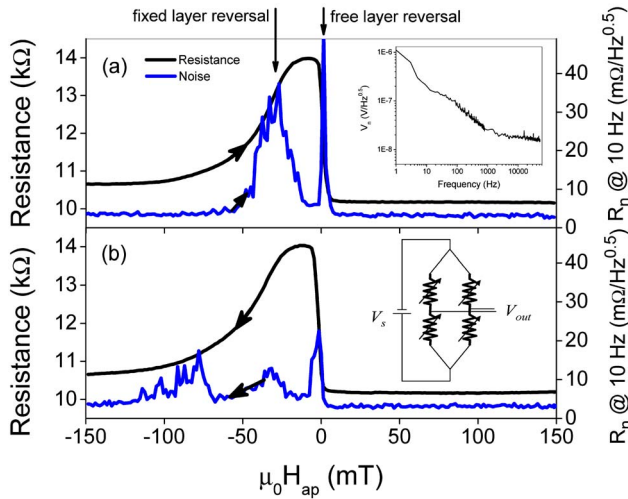


FIG. 1. (Color online) Resistance (V_s divided by the total current passing through the bridge) of a symmetric MTJ bridge that consists of 64 (16 MTJs per bridge leg) $10 \times 20 \mu\text{m}$ MTJs vs applied magnetic field: (a) positive- and (b) negative-going branches. Data on the resistance noise of the MTJ bridge for both positive- and negative-going branches are also plotted at 10 Hz. The insets show (a) the noise spectra V_n obtained by taking the average of the Fourier transform magnitude of $V_{\text{out}}(t)$ at zero applied field and (b) the measurement geometry—see Ref. 16.

$V_s=1$ V). The peaks in the resistance noise are due to thermally activated fluctuations of the magnetization at the tunnel barrier interface. Noise due to environmental magnetic field fluctuations was eliminated by use of a symmetric bridge, which is largely immune to environmental field noise, and by measuring in a shielded environment with low-noise field sources. Peaks in the low-frequency noise are seen in regions of the free layer reversal and the pinned layer reversal. The noise peaks are considerably larger when the sample starts with the pinned layer antiparallel to its pinned direction than when the sample starts with the pinned layer oriented parallel to its pinned direction. The defects giving rise to low-frequency magnetization noise are thought to be associated with the magnetization ripple induced in the free layer by disorder in the pinned layer.¹³

Figures 2(a)–2(c) compare the magnetic field dependence of the quasistatic magnetization M , FMR f_0 , and the

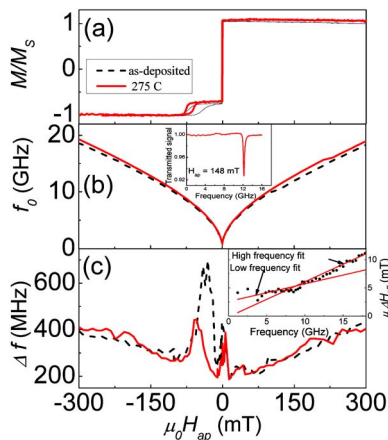


FIG. 2. (Color online) Magnetic field dependence of (a) magnetization, (b) FMR frequency, and (c) linewidth for the as-deposited and 275 °C annealed MTJs. The inset to (b) shows a frequency swept FMR spectra (imaginary part of the normalized transmitted signal) for the 275 °C annealed MTJ at $\mu_0 H_{\text{ap}}=148$ mT. The inset to (c) shows fits to the effective field-swept linewidth data for the as-deposited MTJ.

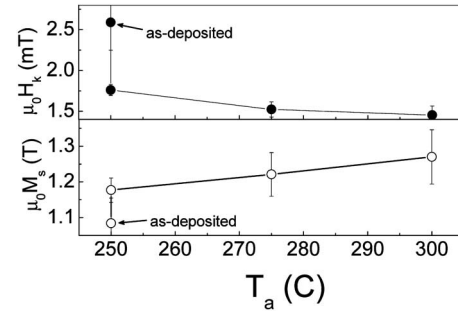


FIG. 3. Anisotropy field H_k and saturation magnetization M_s as functions of annealing temperature determined from the fits of the FMR frequency vs magnetic field data. Data for the as-deposited MTJs, which are heated to 250 °C in the vacuum chamber, are also plotted.

FMR frequency swept linewidth Δf for the as-deposited and 275 °C annealed MTJ samples. As seen from the figures the annealing process changes a number of junction characteristics. The $M(H_{\text{ap}})$ curves show that the annealing procedure sharpens the pinned layer switching and pushes the switching to higher fields. Peaks in the free-layer linewidths are seen that are associated with the reversal of the pinned layer. After annealing, the increase in linewidth during reversal of the pinned layer is diminished, and the peak in the linewidth tracks the increase in switching field. A peak is also observed near the free layer reversal at low fields. There is a small reduction in this peak amplitude and a shift toward zero field after annealing.

Differences in the magnetization curves and in the curvature of the FMR frequency versus magnetic field are seen after annealing [Figs. 2(a) and 2(b)], due to changes in saturation magnetization M_s and anisotropy field H_k , Fig. 3 plots the measured M_s and H_k values as functions of annealing temperature. These parameters were obtained by fitting the resonance frequency versus magnetic field [Fig. 2(b)] to the Kittel equation $f_0=(\gamma\mu_0/2\pi)[(H_k+M_s+H_{\text{ap}})(H_k+H_{\text{ap}})]^{1/2}$, where $\gamma=1.76 \times 10^{11} \text{ s}^{-1} \text{ T}^{-1}$ is the gyromagnetic ratio. Annealing decreases the anisotropy field and increases the saturation magnetization. The bulk of the free layer anisotropy arises from the coupling of the pinned layer and the free layer and reduction in anisotropy with annealing indicates a reduction in this coupling. The increase in magnetization may be due to the getting of oxygen by the barrier and a subsequent increase in the magnetic moment of the adjacent layers. There is a significant change between the as-deposited sample, which undergoes a 250 °C *in situ* annealing and the same sample after an additional *ex situ* 250 °C annealing. This may be due to the increased annealing time, a small error in the *in situ* temperature measurement, or the larger field used in the *ex situ* annealings.

The positive field region of the linewidth can be fitted using a model that assumes that the frequency swept linewidth is a sum of extrinsic broadening and intrinsic damping, multiplied by the change in resonant frequency with applied field:¹² $\Delta f=(\mu_0 H_0+4\pi\alpha f_0/\gamma)df_0/\mu_0 dH_{\text{ap}}$, where α is the Gilbert damping parameter, H_0 is a measure of the variation in the local anisotropy field, and $df_0/\mu_0 dH_{\text{ap}}=(\gamma/2\pi)\sqrt{1+(\gamma\mu_0 M_s/4\pi f_0)^2}$. It is more convenient to fit a calculated effective field-swept linewidth $\mu_0 \Delta H_{\text{eff}} \equiv \Delta f/(df_0/\mu_0 dH_{\text{ap}})=\mu_0 H_0+4\pi\alpha f_0/\gamma$, since this should be a linear function of the resonant frequency and should normalize out the increase in Δf observed near zero frequency due

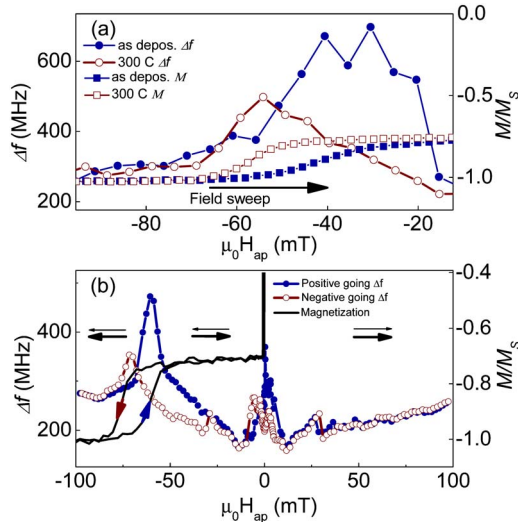


FIG. 4. (Color online) (a) Comparison of magnetization loops and free-layer linewidths in the region corresponding to the switching of the pinned layer for as-deposited and 300 °C annealed MTJs. The solid arrow indicates the direction of the magnetic field sweep for all of the curves. (b) Correlation between the quasistatic magnetization loop and the linewidth for the 275 °C annealed sample. Both positive-going and negative-going curves are shown. The horizontal thin and thick arrows represent the directions of the free and pinned layer, respectively.

to the large change in resonance frequency with small changes in the local anisotropy field (dispersion effects).

We note that ΔH_{eff} is not identical to a measured field-swept linewidth and is a better method for characterizing MTJ devices. In a true field-swept linewidth measurement, the magnetic structure of the device changes during the field sweep and makes the resulting linewidth difficult to interpret. Fits to effective field swept linewidth as a function of resonant frequency are shown in the inset of Fig. 2(c). The slope and intercept yield the values of α and H_0 , respectively. ΔH_{eff} is not linear with resonant frequency, but instead increases significantly at low frequencies. This indicates that the increases in the linewidth do not solely result from static disorder and dispersion effects and a more realistic model of the disorder is needed to describe the data.¹⁴ The values of α and H_0 obtained from fitting the positive low-field region from 1 to 100 mT (f_0 up to 10 GHz) yield $\alpha = 0.0055 \pm 0.0005$ and $H_0 = 2.2 \pm 0.5$ mT for the MTJ films. The sensitivity of α and H_0 to the selected fitting range makes quantitative comparison of these parameters for the different annealing procedures difficult. However, the linear fits show a consistent decrease in the disorder parameter H_0 of approximately 0.3 mT after the additional annealing.

A detailed comparison between the field-dependent magnetization and the linewidth reveals a strong correlation between these quasistatic and dynamic characteristics. In Fig. 4(a) we show the behavior of the as-deposited and 300 °C annealed MTJs near the region of the pinned layer reversal

for the positive-going field sweep. The data show an increase in the sharpness of the pinned layer reversal and a decrease in the amplitude of the linewidth peak upon *ex situ* annealing, which results from a decrease in disorder within the pinned layer. During its reversal, the pinned layer provides a strong inhomogeneous magnetostatic field acting on the free layer, which in turn gives rise to a large extrinsic linewidth. Decreasing the disorder in the pinned layer decreases these extrinsic linewidth broadening mechanisms and results in the observed decreased linewidth, as has been seen in other disordered systems.¹⁵ Figure 4(b) shows the correlation between the linewidth and the quasistatic magnetization for the 275 °C annealed sample in more detail. Here both the positive- and negative-going branches of the field sweep are shown. The increase in the linewidth is larger during the positive-going sweep, which corresponds to starting with the pinned layer in its unfavorable orientation. This is similar to the low-frequency noise spectra and indicates that when the pinned layer starts out oriented in a direction opposite to its pinned direction, more disorder occurs during the reversal process.

In summary, we found a correlation between the regions of increased FMR free-layer linewidth and (1) the reversal regions of the free and pinned layer determined by quasistatic magnetization measurements, (2) the regions of excess $1/f$ noise, and (3) the regions of large magnetization ripple. The regions of increased linewidth, as well as the regions of increased $1/f$ noise, are history dependent, i.e., depend on the starting state of the MTJ. Upon annealing, the peak in linewidth near the reversal of the pinned layer dramatically decreases and sharpens, while in the region of the free-layer reversal, there is a modest decrease in disorder after annealing. The increase in FMR linewidth is a simple method for monitoring the disordered magnetic structure and the improvement created by the annealing process. Hence, the study of FMR linewidth of MTJs may be a useful diagnostic of the quality of the MTJs being developed for a variety of applications.

¹S. Mao *et al.*, *IEEE Trans. Magn.* **38**, 78 (2002).

²P. P. Freitas *et al.*, *J. Phys.: Condens. Matter* **19**, 165221 (2007).

³R. W. Dave *et al.*, *IEEE Trans. Magn.* **42**, 1935 (2006).

⁴A. A. Tulapurkar *et al.*, *Nature (London)* **438**, 239 (2005).

⁵S. Ikeda *et al.*, *IEEE Trans. Electron Devices* **54**, 991 (2007).

⁶C. E. Patton *et al.*, *J. Appl. Phys.* **38**, 1358 (1967).

⁷B. Heinrich *et al.*, *Phys. Rev. Lett.* **90**, 187601 (2003).

⁸R. D. McMichael *et al.*, *J. Appl. Phys.* **83**, 7037 (1998).

⁹L. Lagae *et al.*, *J. Magn. Magn. Mater.* **286**, 291 (2005).

¹⁰J. Z. Sun, *Phys. Rev. B* **62**, 570 (2001).

¹¹J.-V. Kim, *Phys. Rev. B* **73**, 174412 (2006).

¹²S. S. Kalarickal *et al.*, *J. Appl. Phys.* **99**, 093909 (2006).

¹³J. M. Shaw *et al.*, *Appl. Phys. Lett.* **89**, 212503 (2006).

¹⁴R. D. McMichael, *J. Appl. Phys.* **103**, 07B114 (2008).

¹⁵R. D. McMichael *et al.*, *J. Appl. Phys.* **91**, 8659 (2002).

¹⁶N. A. Stutzke *et al.*, *J. Appl. Phys.* **97**, 10Q107 (2005).